EPJ manuscript No.
(will be inserted by the editor)

0-π oscillations in nanostructured Nb/Fe/Nb Josephson junctions

Samanta Piano[1,2], J. W. A. Robinson[1], Gavin Burnell[3], and Mark G. Blamire[1]

[1] Department of Materials Science, University of Cambridge - Pembroke Street, Cambridge CB2 3QZ, UK

[2] Physics Department, CNR-Supermat Laboratory, University of Salerno - Via S. Allende, 84081 Baronissi (SA), Italy

[3] School of Physics and Astronomy, E.C. Stoner Laboratory, University of Leeds - Leeds, LS2 9JT, UK

Received: date / Revised version: date

Abstract. The physics of the π phase shift in ferromagnetic Josephson junctions may enable a range of applications for spin-electronic devices and quantum computing. We investigate transitions from "0" to "π" states in Nb/Fe/Nb Josephson junctions by varying the Fe barrier thickness from 0.5 nm to 5.5 nm. From magnetic measurements we estimate for Fe a magnetic dead layer of about 1.1 nm. By fitting the characteristic voltage oscillations with existing theoretical models we extrapolate an exchange energy of 256 meV, a Fermi velocity of 1.98×10^5 m/s and an electron mean free path of 6.2 nm, in agreement with other reported values. From the temperature dependence of the $I_C R_N$ product we show that its decay rate exhibits a nonmonotonic oscillatory behavior with the Fe barrier thickness.

PACS. 74.50.+r Tunneling phenomena; point contacts, weak links, Josephson effects – 74.25.Sv Critical currents – 74.78.Db Low-Tc films – 74.25.Ha Magnetic properties

1 Introduction

In recent years a great interest has grown in the implementation of quantum computing [1], where information is stored in two-level quantum systems (qubits). Many theoretical and experimental advances have been achieved towards the physical realisation of qubits and, in this respect, solid-state implementations appear as good candidates thanks to their potential scalability which is partly enabled by the development of nano-scale technology [2]. In particular, ferromagnetic π-junctions have been proposed as coherent two-state quantum systems [3]. In a Superconductor/Ferromagnet (S/F) system the superconducting order parameter penetrates into the F layer. As a consequence of exchange splitting of the spin-up and spin-down electrons in the ferromagnetic sub-bands the superconducting order parameter oscillates as a function of depth in the F-layer which causes its sign to change pe-

riodically [4,5,6]. A positive order parameter corresponds to a "0"-state, while a negative order parameter to a "π"-state. To realise a practical quantum device it is necessary to control these two states; this is easily achieved in S/F/S systems incorporating weak [7] and strong [8,9,10] F barriers and hence such systems have been identified as suitable quantum-electronic devices based on π-shift technology [11]. These systems exhibit oscillations of the critical current with F layer thickness equivalent to a change of phase from 0 to π-states. The principle goal in this research field is to understand the physics of superconductor based quantum technology and to evaluate potential material systems, while aiming at reducing the size of the employed heterostructures towards the nano-scale.

In this paper, we present the first study of the thickness dependence of the critical current oscillations in niobium/iron/niobium (Nb/Fe/Nb) Josephson junctions. Magnetic measurements as a function of the Fe layer thickness (t_{Fe}) have been made so that an estimate of the magnetic dead layer of our Fe barrier layer can be obtained. The current *vs* voltage characteristics have been measured for different thicknesses of the Fe and show periodic transitions from 0-states to π-states from nodes in the $I_cR_N(t_{Fe})$ relation, where I_c is the critical current of the device and R_N is the normal-state resistance. From a comparison between experimental data and two theoretical models we have estimated the exchange energy and the Fermi velocity of the Fe barrier, which are found to be in good agreement with the expected values from literature. With a simple model we estimate the mean free path of Fe verifying that the clean limit condition is fulfilled. From the study of the temperature dependence of the I_CR_N product we have shown that its decay rate exhibits a nonmonotonic oscillatory behavior with the Fe barrier thickness. Our analysis reveals that Fe, for its small magnetic dead layer and high exchange energy, is well-suited for the implementation into nano-scale superconductor based quantum electronics.

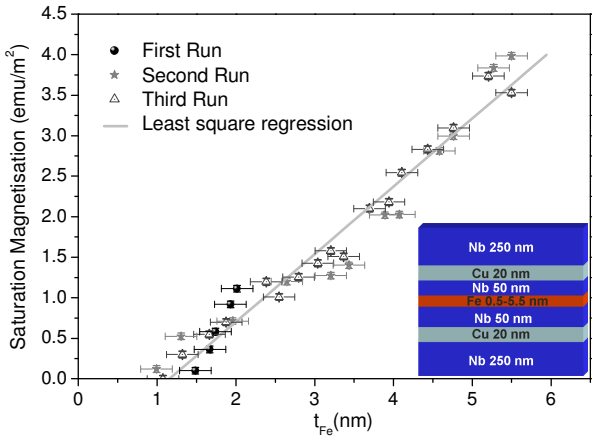

Fig. 1. (Colour online) Saturation magnetisation *vs.* Fe barrier thickness for three deposition runs. The measurements were taken at room temperature. From the linear fit the magnetic dead layer is extrapolated. Inset: illustration of our multilayers.

2 Magnetic properties of Nb/Fe/Nb

Our heterostructures consist of Nb (250 nm) / Fe (0.5 nm - 5.5 nm) / Nb (250 nm). To assist subsequent processing in a focused ion beam (FIB) microscope, 20 nm of Cu was deposited inside the outer Nb electrodes, but 50 nm away from the Fe barrier. We remark that the 20 nm of Cu is a thickness smaller than its coherence length, so it is completely proximitised into the Nb, and does not affect the transport properties of the Josephson junction. The

heterostructures are deposited by d.c. magnetron sputtering in an Ar plasma at 1.5 Pa on 10×5 mm silicon (100) substrates coated with a 250 nm thick oxide layer on the surface. Our deposition system is equipped with a rotating holder which can move under three magnetrons and allows the loading of more than twenty substrates in one run. In this way our system permits, knowing the relation between the deposition rate and the speed of the rotating holder, to deposit *in-situ* and in a single run, different samples with various Fe barrier thicknesses. From x-ray reflectivity measurements, we have verified the control of Fe barrier thickness variation t_{Fe} to be within an accuracy of ± 0.2 nm [12].

To investigate the magnetic properties of our devices we have measured, using a vibrating sample magnetometer at room temperature, the magnetic moment per unit surface area of the films as a function of Fe barrier thickness. The saturation magnetisation was measured for three different deposition runs (see Fig. 1), where for each deposition we have obtained similar saturation magnetisations which also confirms our control of the Fe barrier thickness. By extrapolating the least-squares fit of this data we have estimated that the Fe has a magnetic dead layer $t_D \simeq 1.1$ nm. The thickness of the magnetic dead layer is one of the central points into the realisation of quantum devices because it marks the lower limit of the ferromagnetic barrier thickness for which it exhibits magnetic moment. We remark that the scale of the estimated Fe barrier magnetic dead layer is low; however, there is a need for deposition optimisation to minimise the scale of the magnetic dead layer so that better control and tunability of the Nb phase-state is possible. The issues associated with a magnetic dead layer are a particular problem with the strong ferromagnetic barriers because of the very thin layers that have to be deposited in order to exploit or even see π-shift physics and hence, improved accessibility and knowledge of this dead layer is important if strong ferromagnetic materials are to be incorporated into π-shift based technologies.

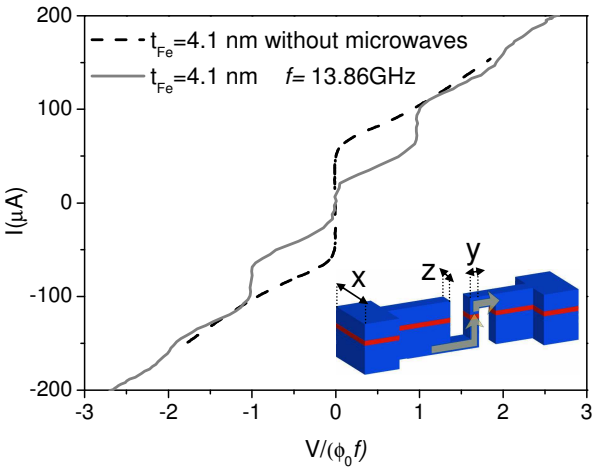

Fig. 2. (Colour online) I *vs.* $V/(\phi_0 f)$, where $\phi_0 = h/2e$, for a Josephson junction with an Fe barrier thickness of 4.1 nm (black dash line) and the same device with 13.86 GHz excitation of microwaves (red line) at T= 4.2 K. Inset: an illustration of a focused ion beam processed device where $x \approx 4\mu$m, $100 \leq y \leq 500$ nm and $100 \leq z \leq 500$ nm. The current path is also shown.

3 Realization of nanostructured Josephson junctions and electrical characterization

The Josephson junctions were fabricated in three steps: (i) patterning of films using optical lithography to de-

fine micron-scale tracks and contact pads. Our mask permits 14 devices per sample which allows us to measure numerous devices and to derive good estimates of important parameters, like I_cR_N; (ii) broad beam Ar ion milling (3 mAcm^{-2}, 500 V beam) to remove unwanted material from around the mask pattern which leaves 4μm tracks for subsequent FIB work; (iii) FIB etching of micron-scale tracts[13] to achieve vertical transport with a device area (yz) in the range 0.2 μm^2 to 1.1 μm^2. We show a labeled illustration of a device in the inset of Fig. 2.

Transport measurements were made in a custom made liquid He dip probe with a heating stage and microwave antenna fitted. Measurements were made with a standard lock-in technique. The critical current I_c was found from the differential resistance as the point where the differential resistance increases above the value for zero bias current. R_N was measured using a quasi-dc bias current of 3-5 mA, this enabled the nonlinear portion of the I-V curves to be neglected, but was not large enough to drive the Nb electrodes into a normal state.

In Fig. 2 we show I_cR_N *vs.* $V/\phi_0 f$ for a device with an Fe barrier thickness of $\simeq 0.8$ nm with and without microwaves applied, where ϕ_0 is the flux quantum given by $h/2e$ and f is the applied microwave frequency ($f = 14.01$ GHz). Constant voltage Shapiro steps appear due to the synchronisation of the Josephson oscillations on the applied excitation [14] at voltages equal to integer multiples of $hf/2e = 0.029$ meV.

4 Critical current oscillations

For each sample we have measured, from the $I-V$ characteristics, at least three junctions from which the critical current (I_c) and the normal resistance (R_N) of a device is extracted. The I_cR_N product is then plotted as a function of Fe barrier thickness and reveals $I_cR_N(t_{Fe})$ decaying with multiple oscillations in the clean limit up to 5 nm (see Fig.3).

The experimental data have been modeled with the following formula[15]:

$$I_cR_N = I_cR_N(t_0)\left|\frac{\sin\frac{t_{Fe}-t_1}{\xi_2}}{\sin\frac{t_1-t_0}{\xi_2}}\right|\exp\left(\frac{t_0-t_{Fe}}{\xi_1}\right), \qquad (1)$$

where t_1 is the Fe thickness corresponding to the first minimum in I_cR_N, $I_cR_N(t_0)$ is the first experimental value of $I_cR_N(t_{Fe})$, and ξ_1 and ξ_2 are the two fitting parameters. We notice that the experimental data are in good agreement with this theoretical model, and from the fit we obtain $\xi_1 = 3.8$ nm and $\xi_2 = 0.25$ nm and a period of the oscillations is $t = 1.6$ nm. Eq. (1) is a general formula that applies to the clean and dirty limits; however, in the clean limit $\xi_2 = v_F\hbar/2E_{ex}$. By assuming the Fermi velocity of Fe is $v_F = 1.98\times10^5$ m/s, as reported in literature[16], we calculate the exchange energy of the Iron: $E_{ex} = \hbar v_F/2t \approx 256$ meV.

To confirm that our oscillations are in the clean limit (meaning that the considered Fe thickness is always smaller than the Fe mean free path), we have modeled our data with a second simplified formula which holds only in this limit [17]:

$$I_cR_N \propto \frac{|\sin(2E_{ex}t_F/\hbar v_f)|}{2E_{ex}t_F/\hbar v_f}, \qquad (2)$$

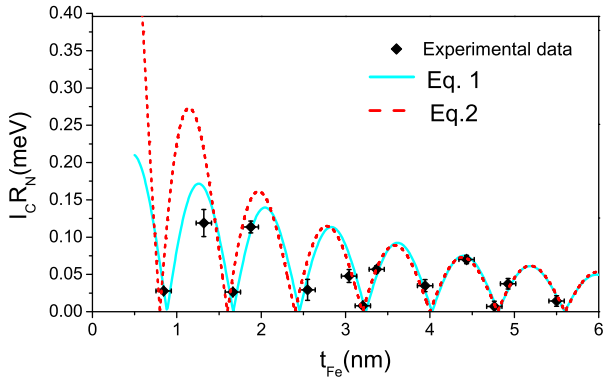

Fig. 3. (Colour online) I_cR_N oscillations as a function of the thickness of the iron barrier (dot) with the theoretical fit (line).

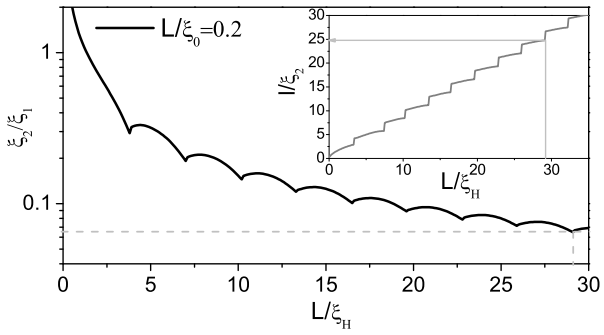

Fig. 4. Dependence of ξ_2/ξ_1 with the inverse magnetic length; inset: L/ξ_H *vs* L/ξ_H to estimate the mean free path, L.

where, in this case, E_{ex} and v_F are the two fitting parameters. From the theoretical fit we extrapolate $E_{ex} = 256$ meV and $v_F = 1.98 \times 10^5$ m/s.

This model is fitted using exactly the same values for the parameters as those obtained from the previous model given by Eq. 1. Both models are thus consistent with one another and show an excellent fit to our data, which exhibit multiple oscillations of I_cR_N in a small range of Fe barrier thickness. In Fig. 3 we show the experimental data with the two theoretical fits. The magnetic dead layer has not been subtracted, as for T= 4K it is expected to be significantly lower than 1.1 nm. This is an important feature towards the realisation of integrated nanostructured quantum electronic devices based on π-phase shift in Nb/Fe/Nb Josephson junctions.

With a simplified model that is obtained solving the linearised Eilenberger equations [18] we can estimate the mean free path of Fe. The general formula is:

$$\tanh \frac{L}{\xi_{eff}} = \frac{\xi_{eff}^{-1}}{\xi_0^{-1} + L^{-1} + i\xi_H^{-1}}, \qquad (3)$$

where ξ_{eff} is the effective decay length given by $\xi_{eff}^{-1} = \xi_1^{-1} + i\xi_2^{-1}$, ξ_o is the Ginzburg-Landau coherence length and ξ_H is a complex coherence length. In the clean limit $1 + L\xi_0^{-1} >> (\max\{\ln(1 + L\xi_0^{-1}), \ln(L\xi_H^{-1})\})/2$. The solution of this equation gives: $\xi_1^{-1} = \xi_0^{-1} + L^{-1}$, $\xi_0 = (v_F\hbar)/(2\pi T_c k_B)$ and $\xi_2 = \xi_H$.

In our case the ratio $\xi_2/\xi_1 \simeq 0.06$, and so assuming L/ξ_0=0.2 we can extrapolate from the graphical solution a value of $L/\xi_H \simeq 29$ (Fig.4). Considering the curve L/ξ_2 *vs* L/ξ_H (inset in Fig.4) we obtain a value of L/ξ_2 to be $\simeq 25$ and hence, we estimate the mean free path of Fe to be $\simeq 6.2$ nm. With this analysis we remark that the condition that $I_cR_N(d_{Fe})$ is within the clean limit only is fulfilled.

We have followed the temperature dependence of the I_CR_N product for different thicknesses of the Fe barrier, as shown in Fig.5. We note that, for each Fe barrier thickness, the Josephson junction resistance remains approximately constant. On the other hand, the critical current, and hence the I_CR_N product, quickly decreases with increasing the temperature. It is interesting to notice how

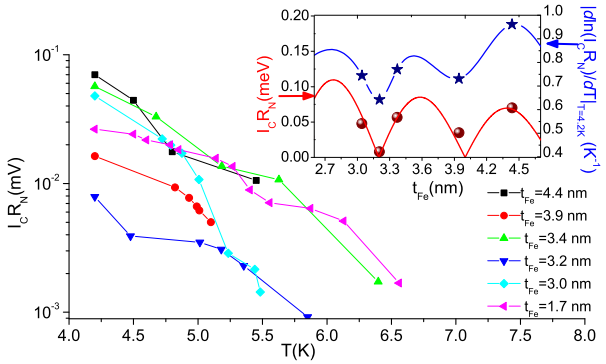

Fig. 5. (Colour online) Temperature dependence of the I_CR_N for different thicknesses of the Fe layer (logarithmic scale). Inset: oscillations of the decay rate $\alpha_T(T_0 = 4.2\text{K})$ of I_CR_N, Eq. (4), with the temperature [stars; the blue line is a guide to the eye], as compared with the oscillations of the I_CR_N product itself [spheres; the red line is the fit given by Eq. (1)] in a window of Fe thicknesses.

the rate at which the critical current drops to zero exhibits a nonmonotonic dependence on the Fe layer thickness. We can define the relative decay rate α_T of the I_CR_N product with the temperature as in Ref. [8], namely

$$\alpha_T(T_0) = \left|\frac{\mathrm{d}\ln[I_CR_N(T)]}{\mathrm{d}T}\right|_{T=T_0} = \left|\frac{\mathrm{d}I_CR_N(T)}{\mathrm{d}T}\right|_{T=T_0} \frac{1}{I_CR_N(T_0)}, \quad (4)$$

calculated at $T_0 = 4.2$ K. In the inset of Fig.5 we plot α_T as a function of t_{Fe} for five consecutive thicknesses; we observe oscillations of α_T in phase with the oscillations of the I_CR_N, in other words the smaller I_CR_N decays to zero with increasing T more slowly than the greater I_CR_N.

5 Conclusions

In summary, we have fabricated Nb/Fe/Nb nano-scale Josephson junctions and investigated the effect of varying the Fe barrier thickness on I_cR_N. From magnetic measurements the Fe barriers were found to have a magnetic dead layer of $\simeq$ 1.1 nm. From $I-V$ curves we have measured the Josephson critical current (I_c) and the normal-state resistance R_N so that oscillations in I_cR_N as a function of the Fe barrier thickness could be studied. In agreement with two theoretical models we have fitted our data and estimated the exchange energy of Fe to be 256 meV and the Fermi velocity of Fe to be 1.98×10^5 m/s. Furthermore, we have applied a simple theoretical model that involves solving the linearised Eilenberger equations so that an estimate of the Fe electron mean free path could be made (6.2 nm). A value of 6.2 nm confirms that $I_cR_N(t_{Fe})$ oscillations are fully in the clean limit giving rise to a maximised I_cR_N product in the π-state. For different Fe barrier thicknesses we have shown that the I_CR_N product decreases with increasing temperature, and in particular the decay rate presents the same oscillatory behavior as the critical current, this original feature seems common to strong ferromagnetic π junctions [12], although no explanation for this can yet be given. With this work we have shown that it is possible to fabricate nanostructured Nb/Fe/Nb π-junctions with a small magnetic dead layer of 1.1 nm and with a high level of control over the Fe barrier thickness variation. The estimated exchange energy of Fe is close to bulk Fe implying that the Fe is clean and S/F roughness is minimal. Some interfacial diffusion of Fe into Nb could account for the slight suppression of $E_{ex}(Fe)$ and the magnitude of the magnetic dead layer. We conclude that Fe barrier S/F/S Josephson junctions are viable structures in

the development of superconductor-based quantum electronic devices. The electrical and magnetic properties of Fe are well understood and are routinely used in the magnetics industry, therefore Nb/Fe/Nb multilayers can readily be used in controllable two-level quantum information systems.

References

1. Nielsen M. A. and Chuang I. L., *Quantum Computation and Quantum Information* (Cambridge University Press, Cambridge, UK) 2000.
2. Doveret M. H., Wallraff A., and Martinis J. M., cond-mat/0411174 (2004).
3. Yamashita T., Tanikawa K., Takahashi S., and Maekawa S., *Phys. Rev. Lett.*, **95** (2005) 097001.
4. Ryazanov V. V., Oboznov V. A., Rusanov A. Y., Veretennikov A. V., Golubov A. A., and Aarts J., *Phys. Rev. Lett.*, **86** (2001) 2427.
5. Kontos T., Aprili M., Lesueur J., and Grison X., *Phys. Rev. Lett.*, **86** (2001) 304.
6. Buzdin A. I., *Rev. Mod. Phys.*, **77** (2005) 935.
7. Kontos T., Aprili M., Lesueur J., Genêt F., Stephanidis B., and Boursier R., *Phys. Rev. Lett.*, **89** (2002) 137007.
8. Blum Y., Tsukernik A., Karpovski M., and Palevski A., *Phys. Rev. Lett.*, **89** (2002) 187004 .
9. Bell C., Loloee R., Burnell G., and Blamire M. G., *Phys. Rev. B*, **71** (2005) 180501(R) .
10. Robinson J. W. A., Piano S., Burnell G., Bell C., and Blamire M. G., *Phys. Rev. Lett.* **97** (2006) 177003 .
11. Yamashita T., Takahashi S., and Maekawa S., *Phys. Rev. B*, **73** (2006) 144517 .
12. Robinson J. W. A., Piano S., Burnell G., Bell C., and Blamire M. G., submitted.
13. Bell C., Burnell G., Kang D.-J., Hadfield R. H., Kappers M. J. and Blamire M. G., *Nanotechnology* **14** (2003) 630.
14. Barone A. and Paternò G., *Physics and Applications of the Josephson effect* (John Wiley & Sons, New York) 1982.
15. Born F., Siegel M., Hollmann E. K., Braak H., Golubov A. A., Gusakova D. Yu. and Kupriyanov M. Yu., *Phys. Rev. B*, **74** (2006) 140501(R).
16. Covo M. K., *et al.*, *Phys. Rev. ST AB*, **9** (2006) 063201.
17. Buzdin A. I., *JETP Lett.*, **35** (1982) 178.
18. Gusakova D. Yu., Kupriyanov M. Yu., and Golubov A. A., *Pisma Zh. Eksp. Teor. Fiz.*, **83** (2006) 487 [*JETP Lett.*, **83** (2006) 418].